Accepted Manuscript

Please cite this article as: Álvarez-Pazos, N., Bravo, J., Graña, A. M., & García-Fontán, S. (2021). Allenylidene and diazoalkane complexes of a half-sandwich mixed phosphine – phosphinite ruthenium fragment. *Inorganica Chimica Acta, 519*, 120277. doi:10.1016/j.ica.2021.120277

Link to published version: https://doi.org/10.1016/j.ica.2021.120277

Allenylidene and diazoalkane complexes of a half-sandwich mixed phosphine-phosphinite ruthenium fragment

Nuria Álvarez-Pazos[a,b], Jorge Bravo[a*], Ana M. Graña[c], and Soledad García-Fontán[a,b*]

[a] Departamento de Química Inorgánica, Universidade de Vigo, Campus Universitario, E-36310 Vigo, Galicia – Spain. [b] Metallosupramolecular Chemistry Group Galicia South Health Research Institute (IIS Galicia Sur) SERGAS-UVIGO. Galicia – Spain. [c] Departamento de Química Física, Universidade de Vigo, Campus Universitario, E-36310 Vigo, Galicia – Spain.

*Corresponding authors
E-mail adress: jbravo@uvigo.gal
sgarcia@uvigo.es

Dedicated to Dr. Maurizio Peruzzini, a great chemist, a better person.

Abstract

Half-sandwich mixed phosphine-phosphinite ruthenium complexes [RuCp'Cl(PPh_3)L] [Cp' = Cp (**1**), Cp* (**2**)], and [RuCp*ClL_2] (**3**) were prepared by substitution of the triphenylphosphine by the phosphinite ligand PPh_2OCH_2Ph, **L**, on the parent complexes [RuCp'Cl(PPh_3)$_2$]. Allenylidene compounds [Ru(η^5-C_5H_5){=C=C=CPh_2}(PPh_3)L][PF_6] (**4**) and [Ru(η^5-C_5Me_5){=C=C=CPhR}(L)(L')][BPh_4] [L' = PPh_3 **(5)**, L **(6)**; R = Ph **(a)**, R = Me **(b)**] were obtained by reaction of compounds **1-3** with the appropriate propargylic alcohols 1,1-diphenyl-2-propyn-1-ol, and 2-phenyl-3-butyn-2-ol. Diazoalkane complexes [RuCp($N_2CAr_1Ar_2$)(PPh_3)L][PF_6] [Ar_1 = Ar_2 = Ph (**7a**), Ar_1Ar_2 = $C_{12}H_8$ (**7b**)] and [RuCp*{$N_2C(C_{12}H_8)$}L_2][PF_6] (**8**) were obtained by reaction of **1** or **3** with the corresponding diazoalkanes in the presence of $NaPF_6$. Complexes were characterized by IR and NMR spectroscopy and, in the case of compounds **1** and **7a**, by X-ray diffraction analysis.

Keywords: Ruthenium; Half-sandwich complexes; Diazo complexes; Allenylidene complexes.

Highlights

Preparation of half-sandwich ruthenium allenylidene complexes.

Preparation of diazoalkane complexes of ruthenium.

The diazoalkane unit presents an important bending angle Ru-N-N.

DFT studies corroborate the role of metal-ligand overlap in the HOMO and lower occupied orbitals to the acute character of the Ru-N-N angle.

1. Introduction

Since allenylidene transition metal complexes were discovered [1], their chemistry has rapidly expanded, especially after the discovery by Selegue of a simple method of synthesis by activation of propargylic alcohols [2]. In recent decades the importance of these compounds has grown significantly due to their applications in organic synthesis both in catalytic and stoichiometric processes [3 and references therein]. Allenylidene complexes are metalahomocumulenes with a very versatile reactivity mainly due to the different nature of the three carbon atoms that make up the allenylidene ligand, $:C_\alpha=C_\beta=C_\gamma R_2$, since while Cα and Cγ are electrophilic, C_β is nucleophilic.

Diazoalkane complexes are metalaheterocumulenes, $:N_\alpha=N_\beta=C_\gamma R_2$ in which the diazoalkane group can mainly coordinate to metals through the N atom by a σ bond in an end-on mode or by a π bond in a side-on mode. The reaction of a transition metal complex with diazoalkanes can lead to a diazoalkane complex or a carbene complex with extrusion of N_2 [4], yielding compounds that can be used as active catalysis in organic synthesis [5][6].

Because the nature of the ancillary ligands has a great influence on the properties of both allenylidene [7] and diazoalkane complexes [8] we have synthetized new half-sandwich ruthenium members of these families bearing the phosphinite ligand Ph_2POCH_2Ph (**L**) to analyze its influence on their properties.

2. Experimental Section

2.1. General Procedures

All synthetic operations were performed under a dry argon atmosphere by following conventional Schlenk techniques. Solvents were purified by distillation from the appropriate drying agents [9] and degassed before use. All reagents were obtained from commercial sources and used as received. Ph_2POCH_2Ph (**L**) [10], $[RuCl(\eta^5\text{-}C_5H_5)(PPh_3)_2]$ [11], and $[RuCl(\eta^5\text{-}C_5Me_5)(PPh_3)_2]$ [12] were synthetized following previously published methods. IR spectra were recorded in KBr pellets on a Jasco FT/ IR (ATR) spectrophotometer. NMR spectra were recorded on a Bruker ARX 400 instrument. Chemical shifts are given in parts per million from $SiMe_4$ (^1H and $^{13}C\{^1H\}$) or 85% H_3PO_4 ($^{31}P\{^1H\}$). ^1H and $^{13}C\{^1H\}$ NMR signal assignments were confirmed by ^1H-COSY and HSQC (^1H-^{13}C) experiments. Elemental analyses were performed on a Carlo Erba 1108 apparatus.

2.2. Synthesis of compounds

2.2.1. $[Ru(\eta^5\text{-}C_5H_5)Cl(PPh_3)(L)]$ ***(1)***

A mixture of $[Ru(\eta^5\text{-}C_5H_5)Cl(PPh_3)_2]$ (0.1 g, 0.13 mmol) and a slight excess of the ligand **L** (45 µL, 0.15 mmol) were refluxed in 10 mL of THF for 30 minutes. The yellow solution obtained was cooled until room temperature and concentrated under reduced pressure giving an orange oil that was treated with pentane (2 × 3 mL) and MeOH (2 × 3 mL). The yellow solid obtained was recristallized from a $CHCl_3$ solution.

Yield: 97%. Anal. Calc. for $C_{42}H_{37}ClOP_2Ru$ (756.21 g/mol): C, 66.70; H, 4.93; Exp.: C, 66.78; H, 4.99 %. ^1H NMR ($CHCl_3$-d_1, 25°C) δ: 7.97–7.05 (m, 30H, Ph), 4.45 (m, 1H, OCH_2), 4.26 (s, 5H, η^5-C_5H_5), 4.22 (m, 1H, OCH_2) ppm; $^{31}P\{^1H\}$ NMR ($CHCl_3$-d_1, 25°C) δ: 140.9 (d), 44.0 (d) ($^2J_{PP}$ = 57.6 Hz) ppm. ^1H NMR (CH_2Cl_2-d_2, 25°C) δ: 7.93–7.02 (m, 30H, Ph), 4.41 (m, 1H, OCH_2), 4.24 (s, 5H, η^5-C_5H_5), 4.21 (m, 1H, OCH_2) ppm; $^{31}P\{^1H\}$ NMR (CH_2Cl_2-d_2, 25°C) δ: 141.2 (d), 44.3 (d) ($^2J_{PP}$ = 58.1 Hz) ppm.

2.2.2. $[Ru(\eta^5\text{-}C_5Me_5)Cl(PPh_3)(L)]$ ***(2)***

45 µL of **L** (0.15 mmol) were added to a solution of $[Ru(\eta^5\text{-}C_5Me_5)Cl(PPh_3)_2]$ (95 mg, 0.12 mmol) in 10 mL of CH_2Cl_2 at −30 °C and stirred for 10 min. Then, the mixture was concentrated under reduced pressure giving an orange oil that was treated with pentane (2 × 3 mL) and MeOH (2 × 3 mL) yielding an orange solid.

Yield: 76%. Anal. Calc. for $C_{47}H_{47}ClOP_2Ru$ (826.34 g/mol): C, 68.31; H, 5.73. Exp.: C, 68.37; H, 5.78. ^{1}H NMR (CH_2Cl_2-d_2, 25°C) δ: 7.85−6.92 (m, 30H, Ph), 4.14 (m 1H, OCH_2), 3.95 (m, 1H, OCH_2), 1.12 (t, $^4J_{HP}$ = 1.7 Hz, 15 H, η^5-C_5Me_5) ppm; $^{31}P\{^1H\}$ NMR (CH_2Cl_2-d_2, 25°C) δ: 142.1 (d), 43.7 (d) ($^2J_{PP}$ = 57.8 Hz) ppm.

2.2.3. [Ru(η^5-C_5Me_5)Cl(L)$_2$] ***(3)***

An excess of **L** (90 μL, 0.30 mmol) was added to a solution of [Ru(η^5-C_5Me_5)Cl(PPh_3)$_2$] (95 mg, 0.12 mmol) in 10 mL of CH_2Cl_2 and stirred for 1h at room temperature. Then, the mixture was concentrated under reduced pressure giving an orange oil that was treated with pentane (3 × 3 mL) yielding an orange solid.

Yield: 65%. Anal. Calc for $C_{48}H_{49}ClO_2P_2Ru$ (856.37 g/mol): C, 67.32; H, 5.76. Exp.: C, 67.55; H, 5.81. ^{1}H NMR (CH_2Cl_2-d_2, 25°C) δ: 7.66–7.03 (m, 30H, Ph), 4.38 (m, 4H, OCH_2), 1.25 (d, $^4J_{HP}$ = 1.5 Hz, 15H, η^5-C_5Me_5) ppm; $^{31}P\{^1H\}$ NMR (CH_2Cl_2-d_2, 25°C) δ: 139.6 (s) ppm.

2.2.4. [Ru(η^5-C_5H_5){=C=C=CPh$_2$}(PPh_3)(L)][PF_6] ***(4)***

To a yellow solution of 50 mg (0.06 mmol) of **1** in 7 mL of MeOH, excess of $NaPF_6$ (51 mg, 0.30 mmol) and 1,1-diphenyl-2-propyn-1-ol (0.33 mmol) were added. The mixture colour changed immediately to dark purple and, after stirring for 15 h, the suspension obtained was filtered through Celite®. The solution obtained was concentrated under reduced pressure giving a purple oil that was treated with pentane (2 × 3 mL) and Et_2O (2 × 2 mL) yielding a purple solid that was filtered and dried under reduced pressure.

Yield: 78%. Anal. Calc. for $C_{57}H_{47}F_6OP_3Ru$ (1055.96 g/mol): C, 64.83; H, 4.48. Exp.: C, 64.70; H, 4.50. IR (ATR): $\nu_{C=C=C}$ 1928 (m) cm^{-1}. ^{1}H NMR (CH_2Cl_2-d_2, 25°C) δ: 7.73–6.56 (m, 40H, Ph), 5.06 (br s, 5H, η^5-C_5H_5), 4.11 (m, 2H, OCH_2) ppm; $^{31}P\{^1H\}$ NMR (CH_2Cl_2-d_2, 25°C) δ: 141.6 (d), 48.1 (d) ($^2J_{PP}$ = 37.5 Hz), –142.3 (sept, J_{PF} = 710.1 Hz, PF_6) ppm; $^{13}C\{^1H\}$ NMR (CH_2Cl_2-d_2, 25°C) δ: 298.2 (t, $^2J_{CP}$ = 18.5 Hz, C_α), 206.5 (br s, C_β), 144.0 (s, C_γ), 137.4–127.0 (Ph), 93.5 (s, η^5- C_5H_5), 70.5 (d, $^2J_{CP}$ = 13.1 Hz, OCH_2) ppm.

2.2.5. [Ru(η^5-C_5Me_5){=C=C=CPhR}(L)(L')][BPh_4] [L' = PPh_3 ***(5)****, L* ***(6)****; R = Ph* ***(a)****, R = Me* ***(b)****]*

To a solution of 0.06 mmol of the corresponding ruthenium precursor (50 mg of **2**, 52 mg of **3**) dissolved in 6 mL of MeOH, 0.32 mmol of $NaBPh_4$ (0.11 g) and 0.32 mmol of

the corresponding alkynol (66.64 mg of 1,1-diphenyl-2-propyn-1-ol, 46.78 mg of 2-phenyl-3- butyn-2-ol). The mixture was stirred for 24 h at room temperature. The dark purple suspension was filtered and the purple solid obtained was washed with Et_2O (2 × 3 mL) and dried under reduced pressure.

(5a) Yield: 65%. Anal. Calc. for $C_{86}H_{77}BOP_2Ru$ (1300.36 g/mol): C, 79.43; H, 5.97. Exp.: C, 79.7; H, 5.87. IR (ATR): $\nu_{C=C=C}$ 1914 (m) cm^{-1}. ^1H RMN (CH_2Cl_2-d_2, 25°C) δ: 7.71- 6.61 (m, 60H, Ph), 4.07 (m, 2H, OCH_2), 1.34 (t, $^2J_{HP}$ = 1.6 Hz, 15 H, η^5-C_5Me_5) ppm; $^{31}P\{^1H\}$ NMR(CH_2Cl_2-d_2, 25°C) δ: 143.6 (d), 49.5 (d) ($^2J_{PP}$ = 40.5 Hz) ppm; $^{13}C\{^1H\}$ NMR (CH_2Cl_2-d_2, 25°C) δ: 299.7 (t, $^2J_{CP}$= 18.3 Hz, C_α), 211.0 (t, $^3J_{CP}$= 2.5 Hz, C_β), 166.1- 122.0 (Ph), 158.9 (s, C_γ), 103.5 (t, $^2J_{CP}$= 2.0 Hz, η^5-C_5Me_5), 70.2 (d, $^2J_{CP}$= 14.5 Hz, OCH_2), 9.9 (s, η^5-C_5Me_5) ppm.

(5b) Yield: 45%. Anal. Calc for $C_{81}H_{75}BOP_2Ru$ (1238.29 g/mol): C, 78.56; H, 6.10. Exp.: C, 78.30; H, 5.98. IR (ATR): $\nu_{C=C=C}$ 1922 (m) cm^{-1}. ^1H NMR (CH_2Cl_2-d_2, 25°C) δ: 8.02- 6.62 (m, 55H, Ph), 4.09 (m, 2H, OCH_2), 2.05 (s, 3H, CH_3), 1.37 (s a, 15 H, η^5-C_5Me_5) ppm; $^{31}P\{^1H\}$ NMR(CH_2Cl_2-d_2, 25°C) δ: 144.3 (d), 51.3 (d) ($^2J_{PP}$= 40.3 Hz) ppm.

(6a) Yield: 60%. Anal. Calc. for $C_{87}H_{79}BO_2P_2Ru$ (1330.38 g/mol): C, 78.54; H, 5.98. Exp.: C, 78.40; H, 6.0. IR (ATR): $\nu_{C=C=C}$ 1916 (m) cm^{-1}. ^1H NMR (CH_2Cl_2-d_2, 25°C) δ: 7.70- 6.85 (m, 60H, Ph), 4.49 (m, 2H, OCH_2), 4.18 (m, 2H, OCH_2), 1.51 (s, 15 H, η^5-C_5Me_5) ppm; $^{31}P\{^1H\}$ NMR(CH_2Cl_2-d_2, 25°C) δ: 148.5 (s) ppm; $^{13}C\{^1H\}$ NMR(CH_2Cl_2-d_2, 25°C) δ: 299.1 (t, $^2J_{CP}$ = 17.9 Hz, C_α), 209.3 (t, $^3J_{CP}$ = 3.1 Hz, C_β), 165.4- 122.2 (Ph), 157.8 (s, C_γ), 104.1 (t, $^2J_{CP}$ = 1.8 Hz,η^5-C_5Me_5), 70.5 (t, $^2J_{CP}$ = 6.3 Hz, OCH_2), 9.9 (s, η^5-C_5Me_5) ppm.

(6b) Yield: 49%. Anal. Calc for $C_{82}H_{77}BO_2P_2Ru$ (1268.31 g/mol): C, 77.65; H, 6.12. Exp.: C, 77.5; H, 6.0. IR (ATR): $\nu_{C=C=C}$ 1927 (m) cm^{-1}. ^1H NMR(CH_2Cl_2-d_2, 25°C) δ: 8.00- 6.85 (m, 55H, Ph), 4.36 (m, 2H, OCH_2), 4.24 (m, 2H, OCH_2), 2.01 (s, 3H, Me), 1.52 (s, 15 H, η^5-C_5Me_5) ppm; $^{31}P\{^1H\}$ NMR (CH_2Cl_2-d_2, 25°C) δ: 147.9 (s) ppm.

*2.2.6. [Ru(η^5-C_5H_5)($N_2CAr_1Ar_2$)(PPh_3)L][PF_6] [Ar_1 = Ar_2 = Ph **(7a)**, Ar_1Ar_2 = $C_{12}H_8$ **(7b)**]*

100 mg (0.13 mmol) of **1**, an excess of the corresponding diazoalkane (0.26 mmol, 75 mg of $C_{13}H_{10}N_2$, 76 mg of $C_{13}H_8N_2$), $NaPF_6$ (44 mg, 0.26 mmol) and 7 mL of EtOH were placed in a Schlenk flask. The mixture was stirred at room temperature for 24 h giving an

orange (**7a**) or green (**7b**) solid that was filtered and washed with EtOH (3 × 2 mL) and dried under reduced pressure. Compound **7a** was crystallised by slow diffusion of EtOH into a CH_2Cl_2 solution of the compound.

(7a) Yield: 80 %. Anal. Calc. for $C_{55}H_{47}F_6N_2OP_3Ru$ (1059.95g/mol): C, 62.32; H, 4.47. Exp.: C, 62.38; H, 4.50. IR (ATR): ν_{N_2} 1931 (m) cm^{-1}. ^1H RMN (CH_2Cl_2-d_2, 25°C) δ: 7.85-6.67 (m, 40H, Ph), 4.79 (s, 5H, η^5-C_5H_5), 4.06 (m, 2H, OCH_2) ppm; $^{31}P\{^1H\}$ NMR (CH_2Cl_2-d_2, 25°C) δ: 142.9 (d), 42.6 (d) ($^2J_{PP}$ = 44.7 Hz), -144.5 (sept, J_{PF} = 710.3 Hz, PF_6) ppm.

(7b) Yield: 78 %. Anal. Calc. for $C_{55}H_{45}F_6N_2OP_3Ru$ (1057.94g/mol): C, 62.44; H, 4.28. Exp.: C, 62.37; H, 4.21. IR (ATR): ν_{N_2} 1942 (m) cm^{-1}. ^1H NMR (CH_2Cl_2-d_2, 25°C) δ: 7.95-6.33 (m, 38H, Ph), 4.93 (s, 5H, η^5-C_5H_5), 4.07 (m, 1H, OCH_2), 3.79 (m, 1H, OCH_2) ppm; $^{31}P\{^1H\}$ NMR (CH_2Cl_2-d_2, 25°C) δ: 141.2 (d), 41.8 (d) ($^2J_{PP}$ = 43.5 Hz), -144.4 (sept, J_{PF} = 710.8 Hz, PF_6) ppm.

2.2.7. [Ru(η^5-C_5Me_5){$N_2C(C_{12}H_8)$}L_2][PF_6] ***(8)***

To a solution of compound **3** (50 mg, 0.05 mmol) in 8 mL of EtOH, an excess of the diazofluorene (24 mg, 0.12 mmol) and $NaPF_6$ (0.13 mg, 0.26 mmol) were added. After stirring for 24 h the solvent was removed under reduced pressure giving an orange solid that was filtered and washed with EtOH (3 × 2 mL) and dried under reduced pressure.

Yield: 78 %. Anal. Calc. for $C_{61}H_{57}F_6N_2O_2P_3Ru$ (1158.26 g/mol): C, 63.20; H, 4.96 Exp.: C, 63.29; H, 5.02. IR (ATR): ν_{N_2} 1928(m) cm^{-1}. ^1H NMR (CH_2Cl_2-d_2, 25°C) δ: 7.99- 6.86 (m, 38H, Ph), 4.36 (m, 4H, OCH_2), 1.48 (s, 15 H, η^5-C_5Me_5) ppm; $^{31}P\{^1H\}$ NMR (CH_2Cl_2-d_2, 25°C) δ: 143.0 (s), -144.4 (sept, J_{PF} = 711.2 Hz, PF_6) ppm.

2.3. Crystal structure determination of [Ru(η^5-C_5H_5)Cl(PPh_3)(L)] ***(1)*** *and [Ru(η^5-C_5H_5)(N_2CPh_2)(PPh_3)L][PF_6]* ***(7a)***

Crystallographic data were collected on Bruker D8 Venture diffractometer at CACTI (Universidade de Vigo) with graphite monochromated Mo Kα radiation (λ = 0.71073 Å) and were corrected for Lorentz and polarization effects. $APEX_3$ [13] software was used for collecting data frames, indexing reflections, and determining lattice parameters, SAINT [14] for integration of intensity of reflections and scaling, and SADABS [15] for empirical absorption correction. The crystallographic treatment of the compounds was performed with the SHELXL97 program [16]. The structure was solved by direct

methods. Non-hydrogen atoms were refined with anisotropic displacement parameters by full-matrix least-squares calculations on F^2 using the program SHELXL with $OLEX_2$ [17]. Hydrogen atoms were calculated in idealized positions and refined with isotropic displacement parameters. The $OLEX_2$ solvent mask routine was used to remove the intensity contributions from the disordered solvent molecules. Details of crystal data and structural refinement are given in Table 1.

Table 1
Crystal data and structure refinement details for compounds **1** and **7a**.

Compound	**1**	**7a**
Empirical formula	$C_{42}H_{37}ClOP_2Ru$	$C_{55}H_{47}F_6N_2O_2P_3Ru$
Formula weight	756.17	1105.99
Temperature (K)	100(2)	100(2)
Wavelength (Å)	0.71073	0.71073
Crystal system	Monoclinic	Monoclinic
Space group	$P2_1/c$	$P2_1/c$
Unit cell dimensions		
a (Å)	15.5766(6)	14.3863(8)
b (Å)	10.8239(4)	18.7028(10)
c (Å)	21.4411(9)	19.0556(10)
α (°)	90	90
β (°)	109.624(2)	99.723(2)
γ (°)	90	90
Volume ($Å^3$)	3405.0(2)	5053.5(5)
Z	4	4
Density (calculated) (Mg/m^3)	1.475	1.454
Absorption coefficient (mm^{-1})	0.667	0.473
F(000)	1552	2272
Crystal size (mm)	0.118 x 0.085 x 0.047	0.216 x 0.142 x 0.066
Θ range for data collection (°)	2.355- 28.340	2.225- 28.358
Index ranges	$-20 \le h \le 20$	$-19 \le h \le 18$
	$-14 \le k \le 14$	$-24 \le k \le 24$
	$-28 \le l \le 28$	$-25 \le l \le 24$
Reflections collected	63648	106161
Independent reflections	8487[R(int)= 0.0580]	12616[R(int)= 0.0448]
Data completeness	0.999	0.999
Absorption Correction	Semi-empirical from equivalents	Semi-empirical from equivalents
Max. and min. transmission	0.7457 y 0.6758	0.7457 y 0.6773
Refinement method	Full-matrix least-squares on F2	Full-matrix least-squares on F2
Data/restraints/parameters	8487 / 0 / 424	12616 / 3 / 696
Goodness-of-fit on F^2	1.037	1.056
Final R indices [I > 2σ(I)]	$R_1 = 0.0319$	$R_1 = 0.0320$
	$wR_2 = 0.0700$	$wR_2 = 0.0670$
R indices (all data)	$R_1 = 0.0465$	$R_1 = 0.0423$

	$wR_2 = 0.0750$	$wR_2 = 0.0704$
Largest diff. peak and hole, e.Å^{-3}	0.788 and -0.989	0.496 and -0.548

2.4. Computational methods

All calculations were performed by using B3LYP method in Gaussian09 [18] with the ECP LANL2DZ basis set for Ru and cv-pVDZ for the remaining atoms. All minima and transition structures were confirmed as critical points by calculating vibrational frequencies.

In order to obtain bond and atomic properties we have performed QTAIM [19] [20] topological electron density analysis on the obtained wavefunctions by using the AIMAll program [21].

3. Results and discussion

3.1. Synthesis of the half-sandwich complexes [Ru(η^5-C_5H_5)Cl(PPh_3)(L)] ***(1)****, [Ru(η^5-C_5Me_5)Cl(PPh_3)(L)]* ***(2)*** *and [Ru(η^5-C_5Me_5)Cl(L)$_2$]* ***(3)***

Complexes **1** - **3** were prepared by substitution of PPh_3 by the phosphinite ligand Ph_2POCH_2Ph from the correspondent precursor complex [RuCp'Cl(PPh_3)$_2$] (Cp' = Cp or Cp*) (Scheme 1). The number of PPh_3 ligands being substituted and the conditions of the substitution depend on the Cp' ligand. So, when Cp' = Cp we were able to substitute only one PPh_3 ligand, no matter the amount of phosphinite ligand nor the temperature of the reaction would be. On the other hand, when Cp' = Cp*, the first PPh_3 ligand is easily substituted at low temperature (-30ºC) using a 1:1 mol ratio of the phosphinite ligand, and when both the ratio and the temperature were increased (see Experimental) both PPh_3 ligands were substituted. We have performed theoretical calculations to shed light on the reasons of the different lability of the PPh_3 ligand in Cp'Ru(PPh_3)$_2$Cl when moving from Cp to Cp* (see below).

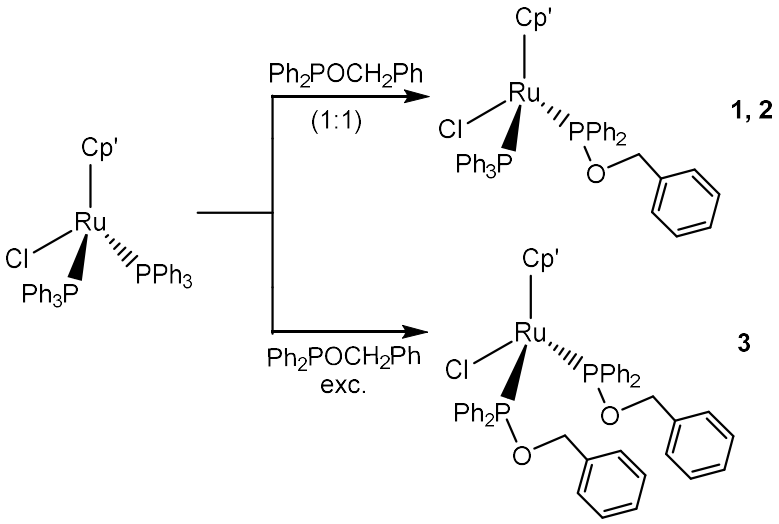

Scheme 1. Synthesis of compounds **1** – **3**, Cp' = Cp (**1**), Cp* (**2**, **3**)

Compounds **1** – **3** were obtained as yellow (**1**) or orange (**2**,**3**) solids stable in air and in solution of common organic solvents. Analytical and spectrocopic data support the proposed formulation. In the ^{1}H NMR spectra of the mixed phosphine-phosphinite **1**,**2** compounds, the methylene protons of the phosphinite ligand **L** give rise to two multiplets (at 4.41 and 4.21 ppm for **1**, and 4.14 and 3.95 ppm for **2**) indicating their diastereotopic nature. The $^{31}P\{^{1}H\}$ NMR spectra display two doublets at 44.3 and 141.2 ppm for **1** (J = 58.1 Hz) and at 43.7 and 142.1 ppm (J = 57.8 Hz) for **2**, corresponding to the phosphine and phosphinite ligands, respectively. On the other hand, the ^{1}H NMR spectrum of the di-phosphinite complex **3** shows only one multiplet at 4.38 ppm assignable to the OCH_2 protons of **L** and the $^{31}P\{^{1}H\}$ NMR spectrum displays one singlet at 139.6 ppm in agreement with the more symmetric environment in this complex. Complex **1** was recrystallised in $CHCl_3$ giving yellow crystals suitable for X-ray diffraction analysis. The compound presents a typical "piano stool" structure (Figure 1) in which the ruthenium atom is surrounded by a pentacoordinated ciclopentadienyl ligand, two P atoms corresponding to the phosphine and phosphinite ligands and a Cl atom. The more relevant bond distances and bond angles are displayed on Table 2. Geometry around Ru atom is a slightly distorted octahedral with the angles between the centroid of the Cp ligand and the legs of the "piano stool" close to the theoretical value (125.3°), and the angles between the legs close to 90°. The Ru-P bond lengths are similar to other half-sandwich ruthenium complexes bearing phosphine and phosphite ligands [22][23][24][25] and significantly differents each other, 2.2634(5) and 2.3053(5) Å, in accordance with the different nature

of both phosphorous ligands, reflecting the more π-accepting capability of the phosphinite ligand compared to the phosphine.

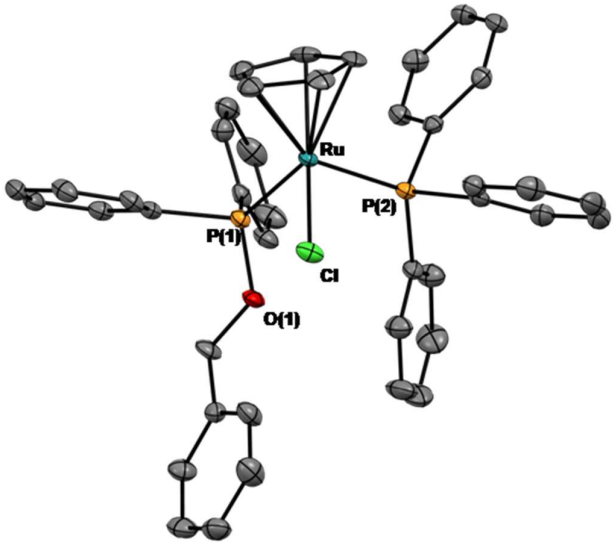

Figure 1. Structure of compound [Ru(η^5-C_5H_5)Cl(PPh_3)L] (**1**). Hydrogen atoms are omitted for clarity.

Table 2

Selected bond distances (Å) and angles (°) for compound **1**.

Ru-CT	1.8633(10)	Ru-P(2)	2.3053(5)
Ru-Cl	2.4445(5)	P(1)-O(1)	1.6194(15)
Ru-P(1)	2.2634(5)	O(1)-C(1)	1.441(2)
CT-Ru-Cl	123.47(3)	Cl-Ru-P(1)	89.321(18)
CT-Ru-P(1)	125.55(4)	Cl-Ru-P(2)	94.132(18)
CT-Ru-P(2)	120.83(4)	P(1)-Ru-P(2)	94.882(19)

CT: Centroid of the Cp ligand

3.2. Theoretical studies

The experimental results shown in the previous paragraph indicate that the nature of the carbocyclic ligand (Cp' = Cp or Cp*) determines the number of phosphine ligands that can be substituted by the phosphinite ligand **L** in the complexes [RuCp'Cl(PPh_3)$_2$]. Figure 2 shows the proposed substitution mechanism, which involves four steps. This mechanism is the same for both molecules. First, one PPh_3 ligand separates from the molecule. Then, the first phosphinite group is incorporated. The third step is the separation of the second PPh_3 ligand and the last one the incorporation of the second phosphinite group.

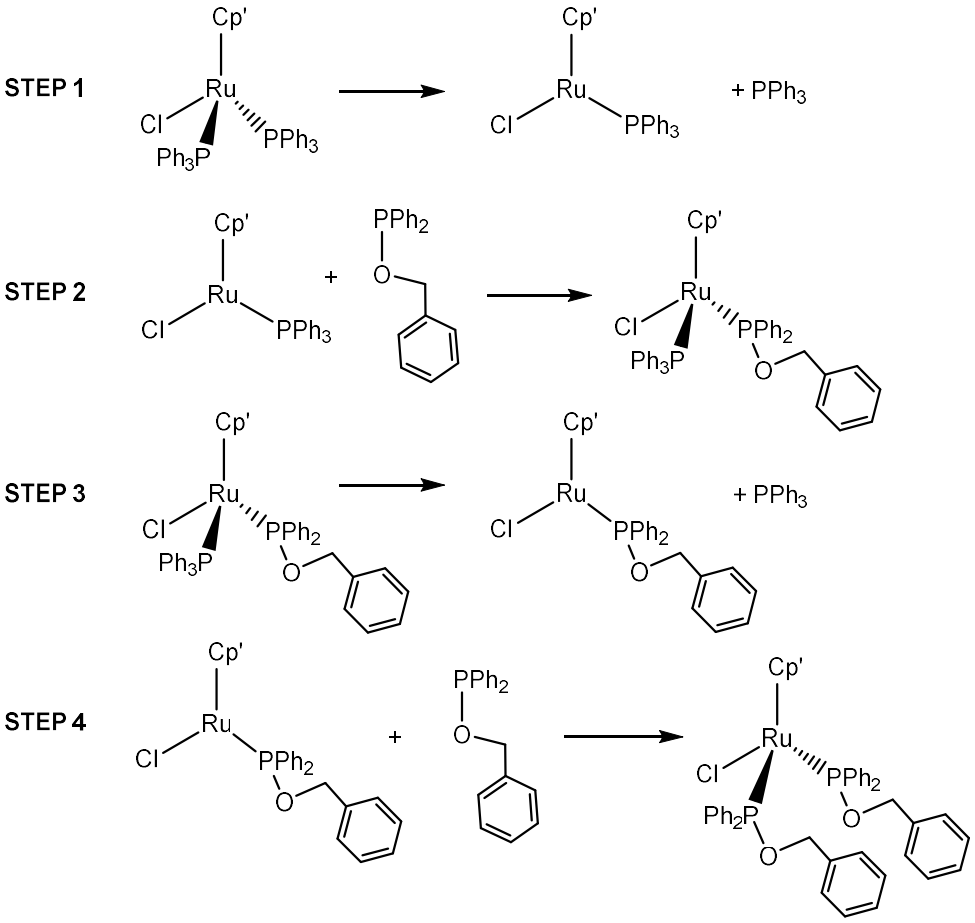

Figure 2. Proposed mechanism for phosphine ligands substitution.

Table 3 contains the values for the energy barriers as well as the differences of energy between reagents and products for every step and for both molecules.

Table 3

Barriers and differences of energy ($\Delta E = E_{products} - E_{reagents}$) in kcal·mol^{-1}

	Molecule	**Step 1**	**Step 2**	**Step 3**	**Step 4**
Barrier	Cp' = Cp	12	1	16	2
	Cp' = Cp*	7	5	3	4
ΔE	Cp' = Cp	11	-16	13	-17
	Cp' = Cp*	-1	-6	2	-9

From Table 3 it could be concluded that when Cp' = Cp* all the steps involve small barriers and the products are more stable than reagents for all the steps except for step 3

for which the difference is only 2 kcal·mol^{-1}. Therefore, this reaction should take place through the four steps quickly. However, when Cp' = Cp, steps 1 and 3 exhibit higher barriers. The highest value corresponds to step 3 and it should be the rate-determining state.

In order to explain the different energy values found for both mechanisms we have also analysed the nature and strength of the bonds involved in the reactions, considering the value of the electron density at the bond critical points, $\rho(r_c)$. We have found that the bonds Ru-P that break during steps 1 and 3 are stronger when Cp' = Cp: $\rho(r_c) = 0.084$ au *vs* $\rho(r_c) = 0.078$ au for step 1 and $\rho(r_c) = 0.085$ au *vs* $\rho(r_c) = 0.078$ au for step 3. All bonds involving Ru (with C, Cl and P atoms) are longer in the reagent of step 3 when Cp' = Cp* so L ligands can avoid the steric effect from methyl substituents of the ring. In addition, the atomic charges of Ru atoms (0.546 au *vs* 0.514 au) and of atoms next to it are smaller in molecule with Cp' = Cp*, also decreasing repulsion effects.

*3.3. Reaction of complexes **1-3** with alkynols. Synthesis of the half-sandwich allenylidene complexes [Ru(η^5-C_5H_5){=C=C=CPh$_2$}(PPh$_3$)(L)][PF$_6$] **(4)** and [Ru(η^5-C_5Me_5){=C=C=CPhR}(L)(L')][BPh$_4$] [L' = PPh$_3$ **(5)**, L **(6)**; R = Ph **(a)**, R = Me **(b)**]*

Transition metal allenylidene complexes can be prepared by reaction of a metallic complex with alkynols via dehydration of a γ-hydroxyvinylidene intermediate [2]. Reaction of complexes **1-3** with alkynols HCCC(OH)Ph$_2$ and HCCC(OH)PhMe in the presence of NaPF$_6$ or NaBPh$_4$, gave the correspondent cationic allenylidene complexes **4 – 6** except for the case of the reaction of **1** with HCCC(OH)PhMe in which a mixture of unidentified products was obtained (Scheme 2). Compounds were obtained as purple solids stable in air but they slowly decompose in solution. The IR spectra of the complexes **4 – 6** show a typical absorption at 1914-1928 cm^{-1} attributable to the $\nu_{C=C=C}$ of the allenylidene ligand [26]. The $^{13}C\{^1H\}$ NMR spectra confirm the presence of this ligand displaying a low-field triplet at 298.2 (**4**), 299.7 (**5a**), and 299.1 (**6a**) attributable to the C_α of the allenylidene chain. Resonances of C_β and C_γ atoms appear at 206.5 (**4**), 211.0 (**5a**), 209.3 (**6a**) and 144.0 (**4**), 158.9 (**5a**), 157.8 (**6a**), respectively. In the case of complexes **5b** and **6b**, their instability in solution precluded running these spectra.

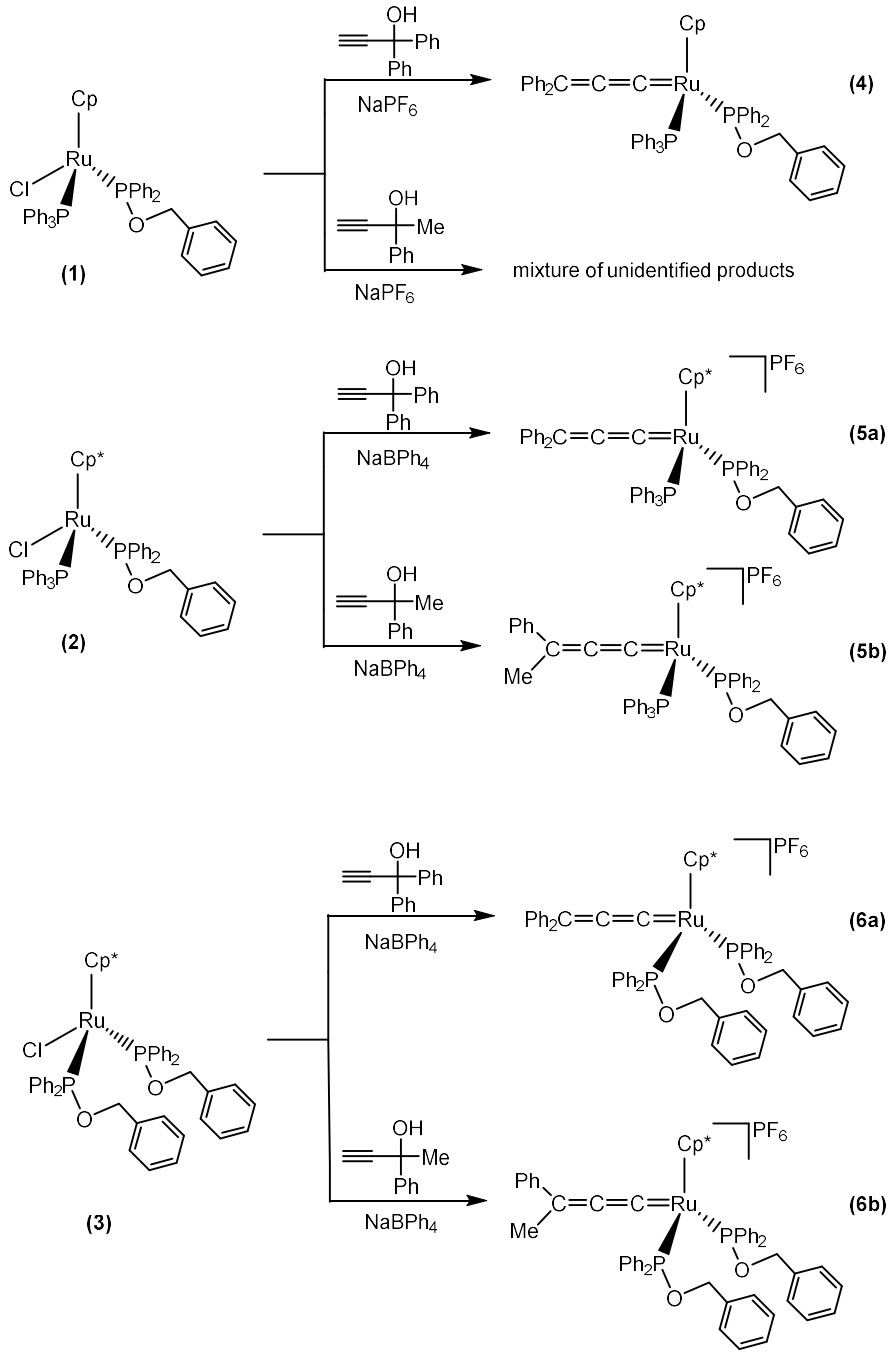

Scheme 2. Synthesis of the allenylidene complexes **4** – **6**.

*3.4. Reaction of complexes **1-3** with diazoalkanes. Synthesis of the half-sandwich diazoalkane complexes [Ru(η^5-C$_5$H$_5$)(N$_2$CAr$_1$Ar$_2$)(PPh$_3$)L][PF$_6$] [Ar$_1$ = Ar$_2$ = Ph **(7a)**, Ar$_1$Ar$_2$ = C$_{12}$H$_8$ **(7b)**] and [Ru(η^5-C$_5$Me$_5$)(N$_2$CAr$_1$Ar$_2$)L$_2$][PF$_6$] [Ar$_1$Ar$_2$ = C$_{12}$H$_8$ **(8)**]*

Diazoalkane complexes $[Ru(\eta^5\text{-}C_5H_5)(N_2CAr_1Ar_2)(PPh_3)L][PF_6]$ (**7**) were obtained, in good yields, by treating half-sandwich compound $[Ru(\eta^5\text{-}C_5H_5)Cl(PPh_3)(L)]$ (**1**) with an excess of the corresponding diazoalkane in the presence of $NaPF_6$, which labilises the Cl^- ligand and facilitates the substitution reaction (Scheme 3).

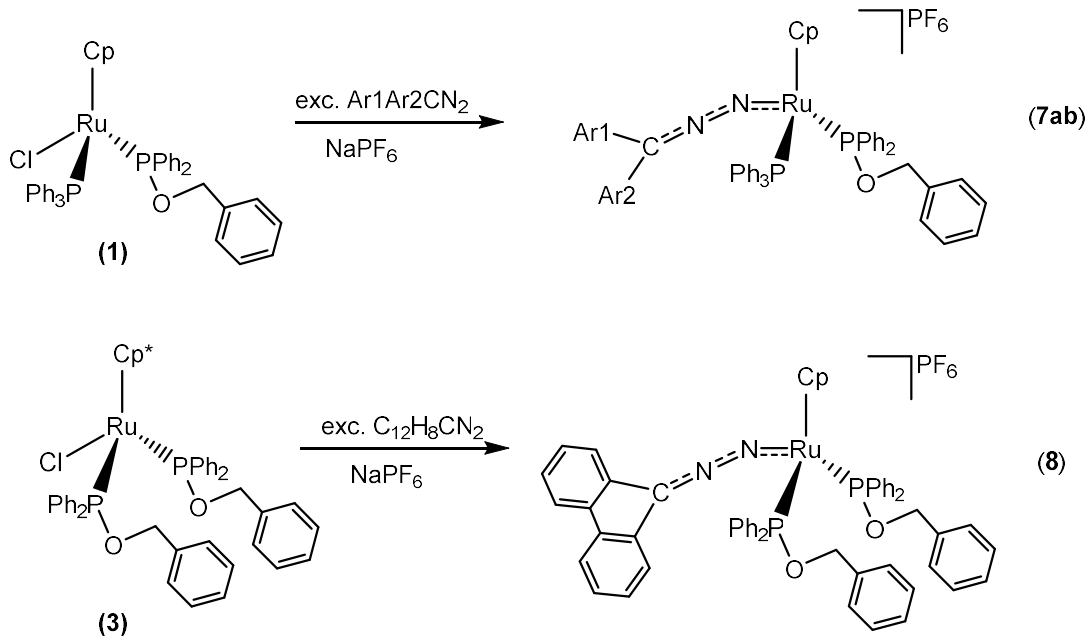

Scheme 3. Synthesis of diazoalkane complexes **7ab** [Ar1 = Ar2 = Ph, (**a**), Ar1Ar2 = $C_{12}H_8$, (**b**)], and **8**.

Complexes **7** were obtained as orange (**7a**) or green (**7b**) solids, stable in air and in common polar organic solvents. Spectroscopic and analytical data support the proposed formulation. The IR spectra shows a medium-intensity band at 1942-1931 cm^{-1} assignable to ν_{N_2} of the diazoalkane group [27]. This value also suggest η^1 coordination mode for the Ar1Ar2CN2 group, similar to that found in the solid state for **7a.** Recrystallisation of compound **7a** by slow diffusion of EtOH into a CH_2Cl_2 solution gave monocrystals suitable for X-ray diffraction analysis. Figure 3 shows the ORTEP view of the cation of compound **7a**, and Table 4 shows selected bond lengths and angles.

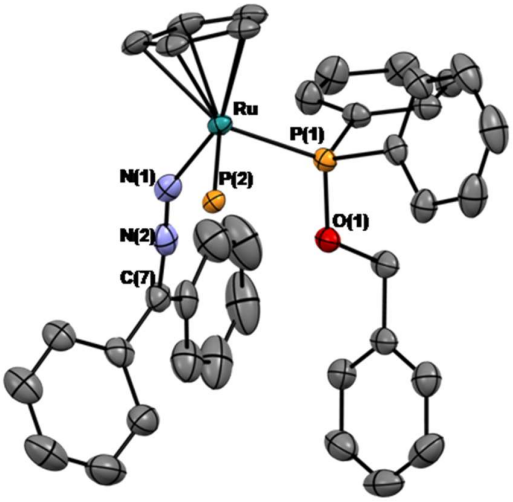

Figure 3. Structure of the cation of compound [Ru(η^5-C_5H_5)(N_2CPh_2)(PPh_3)L][PF_6].EtOH (**7a**). Hydrogen atoms and phenyl rings of the PPh_3 ligand are omitted for clarity.

Table 4

Selected bond distances (Å) and angles (°) for compound [Ru(η^5-C_5H_5)(N_2CPh_2)(PPh_3)L][PF_6].EtOH (**7a**).

Ru-CT	1.8814(9)	Ru-P(2)	2.3364(4)	N(1)-N(2)	1.135(2)
Ru-N(1)	2.0226(16)	P(1)-O(1)	1.6179(12)	N(2)-C(7)	1.314(2)
Ru-P(1)	2.2728(5)	O(1)-C(1)	1.4626(19)		
CT-Ru-N(1)	123.47(5)	N(1)-Ru-P(1)	93.49(4)	Ru-N(1)-N(2)	148.13(13)
CT-Ru-P(1)	122.62(3)	N(1)-Ru-P(2)	93.26(4)	C(7)-N(2)-N(1)	175.74(18)
CT-Ru-P(2)	120.53(3)	P(1)-Ru-P(2)	95.983(16)		

CT: Centroid of the Cp ligand

Compound **7a** consists of an hexafluorophosphate salt of a ruthenium complex in which the ruthenium atom is surrounded by a η^5-Cp ligand, two phosphorous atoms from the phosphine and phosphinite ligands, and the diazo ligand bound to the metal in a η^1 end-on N coordination mode, in a half-sandwich piano-stool structure. The coordination geometry can be considered octahedral being the angles between the centroid of the Cp ligand and the legs (120-123°) and the angles between the legs (93-96°), close to the theoretical values. The Ru-P bond lengths are significantly different, 2.2728(5) and 2.3364(4) Å reflecting the different nature of both phosphorous ligands. The diazoalkane unit configuration is bent with an angle Ru-N(1)-N(2) of 148.13(13)°, shorter than those found for similar diazoruthenium complexes [28]. The optimized angles obtained from

DFT calculations (152º and 172º, respectively) agree with the experimental ones (See Supporting Information). As it was previously proposed [8] the acute character of the Ru-N-N angle could be related to the metal-ligand overlap in the HOMO and lower occupied orbitals showing interaction between the metal and the N-N unit. Specifically, the diazoalkane moiety contributes 79% in the building of the HOMO whereas the metal contribution is only 9%, as compared with 75% and 9% found for $[Ru(Cp)\{N_2C(Ph)(p\text{-}tolyl)\}(PPh_3)\{P(OMe)_3\}]^+$ which exhibits a similar Ru-N-N angle (156º). Also, the contribution to the HOMO-19 of diazoalkane (39%) and metal (15%) orbitals is similar to those found for $[Ru(Cp)\{N_2C(Ph)(p\text{-}tolyl)\}(PPh_3)\{P(OMe)_3\}]^+$: 34% and 15%, respectively.

The N(1)-N(2) distance is 1.135(2) Å, lying between N-N double and triple bond [29] and the Ru-N(1) distance is 2.0226(16) Å, significantly longer than those found for similar complexes [28] suggesting an important contribution of the canonical form [Ru]-N≡N-C to the final configuration of the diazoalkane unit.

The IR spectra of compounds **7ab** show a band at 1931 (**7a**) and 1942 (**7b**) cm^{-1} attributable to the ν_{N2} of the diazenide ligands in agreement with the end-on coordination mode of these ligands [30]. The ^1H NMR spectra show, besides the resonances corresponding to the aromatic protons, a singlet at 4.79 (**7a**) and 4.93 (**7b**) ppm attributed to the Cp ligand and multiplets around 4 ppm attributed to the methylenic protons of the phosphinite ligands. The $^{31}P\{^1H\}$ NMR spectra display two doublets in agreement with an AX system as expected from the different nature of the phosphorous ligands.

In contrast, when Cp* compounds $[Ru(\eta^5\text{-}C_5Me_5)Cl(PPh_3)(L)]$ (**2**) and $[Ru(\eta^5\text{-}C_5Me_5)Cl(L)_2]$ (**3**) were reacted with the same diazoalkanes, the results were different (Scheme 3). In the case of compound **2** we obtained a mixture of unidentified compounds. Reaction of compound **3** with the diazoalkane Ph_2CN_2 also gave decomposition products. However, when compound **3** was reacted with diazofluorene, we were able to isolate the corresponding diazo derivative $[Ru(\eta^5\text{-}C_5Me_5)(N_2CAr_1Ar_2)L_2][PF_6]$ [$Ar_1Ar_2 = C_{12}H_8$ (**8**)] in a good yield.

The IR spectrum shows a band at 1928 cm^{-1} attributable to the ν_{N2} of the diazenide ligand and the ^1H NMR spectrum shows, besides the resonances corresponding to the aromatic protons, a singlet at 1.48 ppm attributed to the methyl groups of the Cp* ligand and a multiplet at 4.36 ppm attributed to the methylenic protons of the phosphinite

ligands. The $^{31}P\{^{1}H\}$ NMR spectrum display a singlet in agreement with the proposed formulation.

When a solution of compound **8** in CH_2Cl_2 is set aside for 24 h, decomposition is observed and yellow crystals corresponding to the azine compound **9** (Scheme 4) were obtained. Formation of azine compounds from diazofluorene complexes was already reported [31].

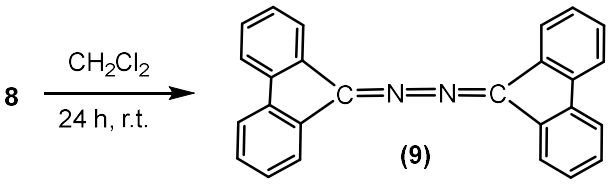

Scheme 4. Obtention of the azine **9** from compound **8**.

4. Conclusions

New half-sandwich ruthenium complexes $[RuCpCl(PPh_3)(L)]$ (**1**), $[RuCp^*Cl(PPh_3)(L)]$ (**2**), and $[RuCp^*Cl(L)_2]$ (**3**), L = (Ph_2POCH_2Ph), were prepared by substitution of PPh_3 ligands by L in $[RuCp'Cl(PPh_3)_2]$, Cp' = Cp, Cp*. Complex $[RuCpCl(L)_2]$ cannot be obtained probably due to the high energy barriers in the substitution process as a DFT study shows. Reaction of complexes **1**-**3** with alkynols HC≡C(OH)(Ph)R, R = Ph, Me gave the corresponding alkynols except for complex **1** and HC≡C(OH)(Ph)(Me) in which case a mixture of unidentified products was obtained. On the other hand, half-sandwich diazoalkane complexes $[Ru(\eta^5\text{-}C_5H_5)(N_2CAr_1Ar_2)(PPh_3)L][PF_6]$ [$Ar_1 = Ar_2 =$ Ph **(7a)**, $Ar_1Ar_2 = C_{12}H_8$ **(7b)**] and $[Ru(\eta^5\text{-}C_5Me_5)(N_2CAr_1Ar_2)L_2][PF_6]$ [$Ar_1Ar_2 = C_{12}H_8$ **(8)**] were obtained by reaction of complexes **1** and **3** with the corresponding diazoalkanes. In the case of complex **7a** suitable crystals for an X-ray diffraction study were obtained. The structure shows an important bending of the Ru-N-N angle, 148.13(13)°, and a DFT study shows that it could be related to the metal-ligand overlap in the HOMO and lower occupied orbitals.

Supporting information

Computational data (cartesian coordinates of compound **7a**): .xyz file; CCDC 2044080 and CCDC 2044081 contain the supplementary crystallographic data for this paper. These data can be obtained free of charge from the Cambridge Crystallographic Data Center via www.ccdc.cam.ac.uk/data_request/cif.

Acknowledgments

Financial support from Xunta de Galicia (Spain) (research ProjectED431D 2017/0) is gratefully acknowledged. We thank the Structural Determination Service of the Universidade de Vigo–CACTI for X-ray diffraction measurements and the collections of NMR data.

References

[1] E.O. Fischer, H.J. Kalder, F.H. Köhler, G. Huttner, Angew. Chem. Int. Ed. Engl. 15 (1976) 623-624.
[2] J.P. Selegue, Organometallics 1 (1982) 217-218.
[3] S. W. Roh, K. Choi, C. Lee, Chem. Rev. 119 (2019) 4293−4356.
[4] M. Dartiguenave, M. J. Menu, E. Deydier, Y. Dartiguenave, H. Siebald, Coord. Chem. Rev. 178–180 (1998) 623–663.
[5] R.R. Schrock, Angew. Chem., Int. Ed. 45 (2006) 3740-3759.
[6] R. H. Grubbs, Angew. Chem., Int. Ed. 45 (2006) 3760-3765.
[7] Metal vinylidenes and allenylidenes in catalysis: from reactivity to applications in synthesis. C. Bruneau, P. Dixneuf Eds. Weinheim: Wiley-VCH (2008).
[8] G. Albertin, S. Antoniutti, M. Bortoluzzi, J. Castro, L. Marzaro, Dalton Trans. 44 (2015) 15470-15480.
[9] D.D. Perrin, W.L.F. Armarego, Purification of Laboratory Chemicals; 3rd ed., Butterworth/Heinemann: London/Oxford, 1998.
[10] K. Masutani, T. Minowa, Y. Hagiwara, T. Mukaiyama, Bull. Chem. Soc. Jpn. 79 (2006) 1106-1117.
[11] M.I. Bruce, C. Hameister, A.G. Swincer, R.C. Wallis, Inorg. Synth. 21 (1982) 78-84.
[12] M.S. Chinn, D.M. Heinekey, J. Am. Chem. Soc. 112 (1990) 5166-5175.
[13] APEX3 (Bruker AXS Inc., 2018).
[14] SAINT Version 6.01, Data Integration Software Package; Bruker Analytical X-Ray Systems Inc., Madison, Wisconsin, USA, 1997.
[15] G.M. Sheldrick, SADABS. A Computer Program for Absorption Corrections. University of Göttingen, Germany (1996).
[16] G.M. Sheldrick, Acta Crystallogr. A, 64 (2008), 112-122.
[17] O.V. Dolomanov, L.J. Bourhis, R.J. Gildea, J.A.K. Howard, H. Puschmann, $OLEX_2$: a complete structure solution, refinement and analysis program, J. Appl. Cryst., 42 (2009) 339-341.
[18] M. J. Frisch, G.W. Trucks, H.B. Schlegel, G.E. Scuseria, M.A. Robb, J.R. Cheeseman, G. Scalmani, V. Barone, B. Mennucci, G.A. Petersson, H. Nakatsuji, M. Caricato, X. Li, H.P. Hratchian, A.F. Izmaylov, J. Bloino, G. Zheng, J.L. Sonnenberg, M. Hada, M. Ehara, K. Toyota, R. Fukuda, J. Hasegawa, M. Ishida, T. Nakajima, Y. Honda, O. Kitao, H. Nakai, T. Vreven, J.A. Montgomery, J.E. Peralta, F. Ogliaro, M. Bearpark, J.J. Heyd, E. Brothers, K.N. Kudin, V. Staroverov, R. Kobayashi, J. Normand, K. Raghavachari, A. Rendell, J.C. Burant, S.S. Iyengar, J. Tomasi, M. Cossi, N. Rega, J.M. Millam, M. Klene, J.E. Knox, J.B. Cross, V. Bakken, C. Adamo, J. Jaramillo, R. Gomperts, R.E. Stratmann, O. Yazyev, A.J. Austin, R. Cammi, C. Pomelli, J.W. Ochterski, R.L. Martin, K. Morokuma, V.G. Zakrzewski, G.A. Voth, P. Salvador, J.J. Dannenberg, S. Dapprich, A.D. Daniels, Ö. Farkas, J.B. Foresman, J.V. Ortiz, J. Cioslowski, D.J. Fox, Gaussian 09; Gaussian, Inc.: Wallingford, CT, 2009.

[19] R. F. W. Bader, Atoms in Molecules; University Press: Oxford, 1990.
[20] R. F. W. Bader, Chem. Rev. 91 (1991) 893-928.
[21] AIMAll (Version 17.11.14), T.A. Keith, TK Gristmill Software, Overland Park KS, USA, 2017 (aim.tkgristmill.com)
[22] G. Albertin, S. Antoniutti, J. Castro, J. Coord. Chem. 72 (2019) 1652-1660.
[23] G. Albertin, S. Antoniutti, M. Bortoluzzi, J. Castro, V. Ferraro, Dalton Trans. 47 (2018) 9173-9184.
[24] G. Albertin, S. Antoniutti, M. Bortoluzzi, A. Botter, J. Castro, Dalton Trans. 44 (2015) 3439-3446.
[25] G. Albertin, S. Antoniutti, A. Botter, J. Castro, Inorg. Chem. 54 (2015) 2091-2093.
[26] S. Bolaño, M.M. Rodríguez-Rocha, J. Bravo, J. Castro, E. Oñate, M. Peruzzini, Organometallics 28 (2009) 6020-6030.
[27] G. Albertin, S. Antoniutti, J. Castro, F. Sibilla, Dalton Trans. 48 (2019) 3116-3131.
[28] G. Albertin, S. Antoniutti, J. Castro, G. Dottorello, Dalton Trans. 44 (2015) 9289-9303.
[29] A.F. Wells, Structural Inorganic Chemistry, 5th ed.; Clarendon Press: Oxford, U.K., 1984.
[30] G. Albertin, S. Antoniutti, M. Bortoluzzi, A. Botter, J. Castro, F. Sibilla, RSC Adv. 6 (2016) 97650-97658, and references therein.
[31] M. Cui, S. Lin, H.H.Y. Sung, I.D. Williams, Z. Lin, Organometallics 38 (2019) 905-915.